



# Coupling of Mitochondrial Import and Export Translocases by Receptor-Mediated Supercomplex Formation

Jian Qiu,<sup>1,2,3,8</sup> Lena-Sophie Wenz,<sup>1,3,8</sup> Ralf M. Zerbes,<sup>1,3</sup> Silke Oeljeklaus,<sup>4,5</sup> Maria Bohnert,<sup>1,4</sup> David A. Stroud,<sup>1,9</sup> Christophe Wirth,<sup>1</sup> Lars Ellenrieder,<sup>1,3</sup> Nicolas Thornton,<sup>1</sup> Stephan Kutik,<sup>1,4</sup> Sebastian Wiese,<sup>4,5</sup> Agnes Schulze-Specking,<sup>1</sup> Nicole Zufall,<sup>1</sup> Agnieszka Chacinska,<sup>6</sup> Bernard Guiard,<sup>7</sup> Carola Hunte,<sup>1,4</sup> Bettina Warscheid,<sup>4,5</sup> Martin van der Laan,<sup>1,4</sup> Nikolaus Pfanner,<sup>1,4,\*</sup> Nils Wiedemann,<sup>1,4,\*</sup> and Thomas Becker<sup>1,4</sup>

<sup>1</sup>Institut für Biochemie und Molekularbiologie, ZBMZ

<sup>2</sup>Spemann Graduate School of Biology and Medicine

<sup>3</sup>Fakultät für Biologie

<sup>4</sup>BIOSS Centre for Biological Signalling Studies

<sup>5</sup>Institut für Biologie II, Fakultät für Biologie, Funktionelle Proteomik

Universität Freiburg, 79104 Freiburg, Germany

<sup>6</sup>International Institute of Molecular and Cell Biology, 02-109 Warsaw, Poland

<sup>7</sup>Centre de Génétique Moléculaire, CNRS, 91190 Gif-sur-Yvette, France

<sup>8</sup>These authors contributed equally to this work

<sup>9</sup>Present address: La Trobe Institute for Molecular Sciences, 3086 Melbourne, Australia

\*Correspondence: [nikolaus.pfanner@biochemie.uni-freiburg.de](mailto:nikolaus.pfanner@biochemie.uni-freiburg.de) (N.P.), [nils.wiedemann@biochemie.uni-freiburg.de](mailto:nils.wiedemann@biochemie.uni-freiburg.de) (N.W.)

<http://dx.doi.org/10.1016/j.cell.2013.06.033>

## SUMMARY

The mitochondrial outer membrane harbors two protein translocases that are essential for cell viability: the translocase of the outer mitochondrial membrane (TOM) and the sorting and assembly machinery (SAM). The precursors of  $\beta$ -barrel proteins use both translocases—TOM for import to the intermembrane space and SAM for export into the outer membrane. It is unknown if the translocases cooperate and where the  $\beta$ -barrel of newly imported proteins is formed. We established a position-specific assay for monitoring  $\beta$ -barrel formation *in vivo* and *in organello* and demonstrated that the  $\beta$ -barrel was formed and membrane inserted while the precursor was bound to SAM.  $\beta$ -barrel formation was inhibited by SAM mutants and, unexpectedly, by mutants of the central import receptor, Tom22. We show that the cytosolic domain of Tom22 links TOM and SAM into a supercomplex, facilitating precursor transfer on the intermembrane space side. Our study reveals receptor-mediated coupling of import and export translocases as a means of precursor channeling.

## INTRODUCTION

Most mitochondrial proteins are synthesized as precursors on cytosolic ribosomes and are imported by the translocase of the outer mitochondrial membrane (TOM) (Dolezal et al., 2006; Neupert and Herrmann, 2007; Schmidt et al., 2010). The outer membrane contains two types of integral membrane proteins:

$\beta$ -barrel proteins and proteins with  $\alpha$ -helical transmembrane segments. The  $\beta$ -barrel protein Tom40 forms the protein-conducting channel of the TOM complex. The complex also contains six proteins that are anchored in the outer membrane by single  $\alpha$ -helical transmembrane segments (Endo and Yamano, 2010; Schmidt et al., 2010; Dukanovic and Rapaport, 2011): three receptor proteins (Tom20, Tom22, and Tom70) that expose domains to the cytosol and recognize the precursor proteins, and three small Tom proteins (Tom5, Tom6, and Tom7) that play roles in the stability and assembly of TOM.

The mitochondrial outer membrane contains a second essential translocase, the sorting and assembly machinery (SAM) (Paschen et al., 2003; Wiedemann et al., 2003; Dolezal et al., 2006; Endo and Yamano, 2010). The SAM (TOB) complex promotes the insertion of  $\beta$ -barrel precursors into the outer membrane. The SAM<sub>core</sub> complex consists of the channel-forming protein Sam50 (Tob55) and two peripheral membrane proteins that expose domains to the cytosol, Sam35 and Sam37. In addition, a fraction of SAM complexes assemble with the  $\beta$ -barrel protein Mdm10 to form the SAM-Mdm10 complex, which is involved in late steps of TOM assembly, including biogenesis of the precursor of Tom22 (Thornton et al., 2010; Endo and Yamano, 2010; Klein et al., 2012).

The outer membranes of Gram-negative bacteria contain a large number of  $\beta$ -barrel proteins. The  $\beta$ -barrel assembly machine (BAM) mediates membrane insertion of  $\beta$ -barrel precursors (Tommassen, 2010; Hagan et al., 2011). According to the endosymbiont hypothesis of mitochondrial origin, Sam50 was derived from BamA of the prokaryotic ancestor of mitochondria, and thus the basic mechanism of  $\beta$ -barrel insertion has been conserved from prokaryotes to eukaryotes (Dolezal et al., 2006; Neupert and Herrmann, 2007; Tommassen, 2010; Hagan et al., 2011; Hewitt et al., 2011). In both bacteria and

mitochondria, the last  $\beta$ -strand of the precursor functions as a signal for the interaction with BAM/SAM (Kutik et al., 2008; Tommassen, 2010). A major difference between prokaryotic and eukaryotic  $\beta$ -barrel biogenesis is the site of synthesis of the precursor proteins. In bacteria, the precursors are synthesized in the cytosol, exported by the Sec machinery, and guided by periplasmic chaperones to the BAM complex (Tommassen, 2010; Hagan et al., 2011; Hewitt et al., 2011). Mitochondrial  $\beta$ -barrel precursors, however, are synthesized outside the organelle. Their biogenesis involves the receptor domains of Tom20, Tom22, and Tom70, and translocation across the outer membrane through TOM (Rapaport and Neupert, 1999; Krimmer et al., 2001; Model et al., 2001; Paschen et al., 2003; Wiedemann et al., 2003; Yamano et al., 2008). The precursors bind to small TIM chaperones of the intermembrane space and are delivered to the SAM complex (Hoppins and Nargang, 2004; Wiedemann et al., 2004). Thus, mitochondrial  $\beta$ -barrel precursors are transported in two opposite directions at the outer membrane: import via TOM and export via SAM. Current models depict TOM and SAM as independent machineries that are not connected (Neupert and Herrmann, 2007; Becker et al., 2009; Endo and Yamano, 2010; Schmidt et al., 2010; Dukanovic and Rapaport, 2011; Hewitt et al., 2011; Shiota et al., 2012). Klein et al. (2012) reported that the complexes do not interact.

Whether folding of the precursor to the native  $\beta$ -barrel occurs before or upon binding of the  $\beta$ -barrel precursor to the BAM/SAM complex, or after its release from the complex, has been the subject of discussion (Neupert and Herrmann, 2007; Endo and Yamano, 2010; Schmidt et al., 2010; Tommassen, 2010; Dukanovic and Rapaport, 2011; Hagan et al., 2011). To analyze  $\beta$ -barrel folding in the native environment, we developed an assay to monitor  $\beta$ -barrel formation in intact mitochondria. We observed that  $\beta$ -barrel folding and membrane insertion occurred in the SAM-bound state. Unexpectedly, the central receptor, Tom22, stimulated  $\beta$ -barrel formation at SAM, revealing a direct connection of TOM and SAM complexes in the biogenesis of  $\beta$ -barrel precursors. This study reveals that receptor-mediated coupling of the two translocases into a supercomplex promotes  $\beta$ -barrel formation, leading to a concept of cooperation of import and export translocases.

## RESULTS

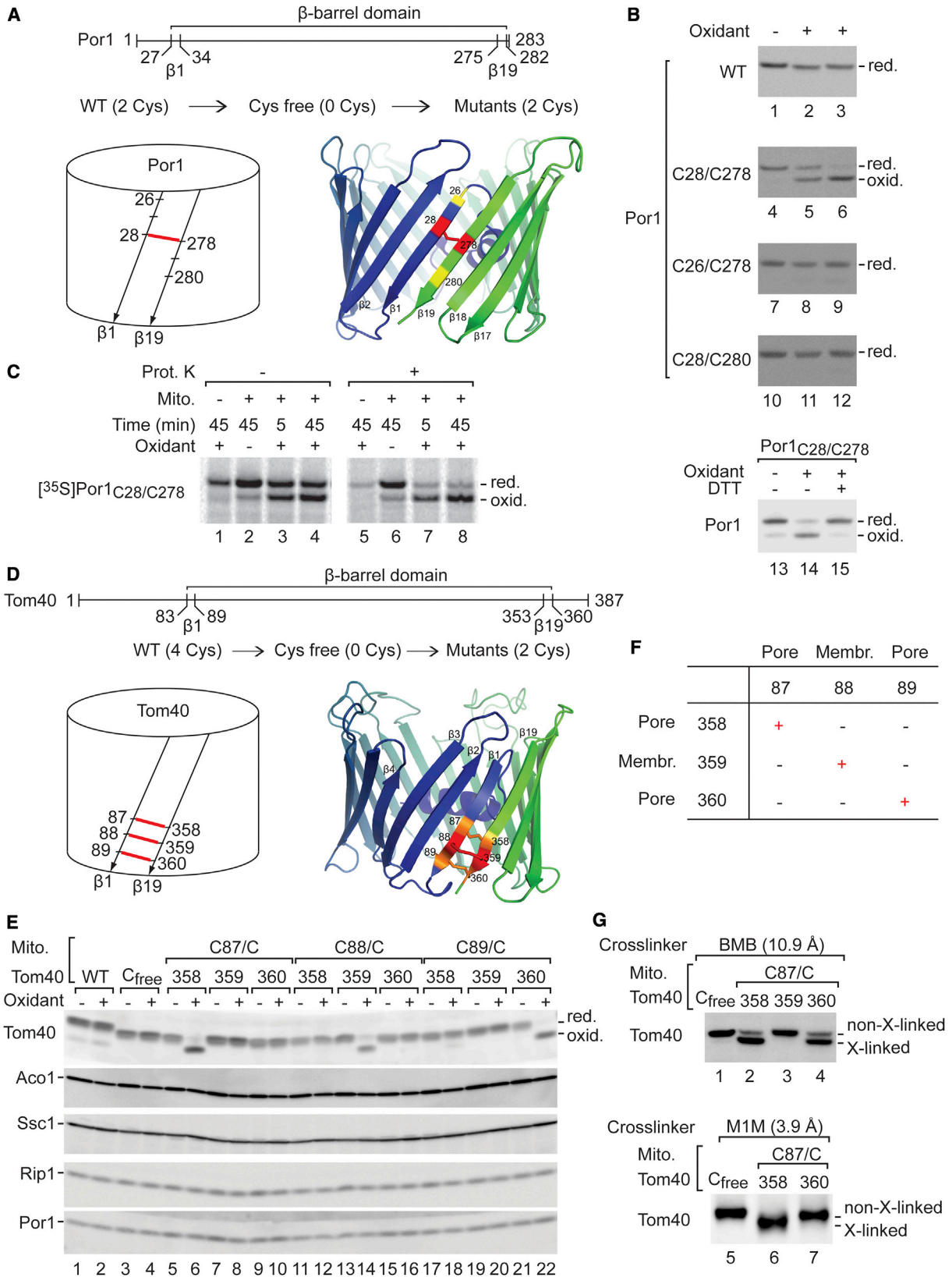
### Monitoring $\beta$ -Barrel Formation In Vivo

To monitor  $\beta$ -barrel formation in intact mitochondria, we used the abundant  $\beta$ -barrel protein porin (Por1, VDAC) as the test substrate. We modeled yeast Por1 according to the structure of mammalian porin as a 19-stranded  $\beta$ -barrel and generated mutant forms that contained two cysteines, one in  $\beta$ -strand 1 and one in  $\beta$ -strand 19 (Figure 1A; Figure S1A available online). All mutant strains grew like wild-type (WT) cells (Figure S1B). When the cysteines were in directly adjacent positions (residues 28 and 278), treatment of the mitochondria with oxidants generated a faster-migrating form on nonreducing SDS-PAGE (Figure 1B). Treatment with the reducing agent dithiothreitol (DTT) regenerated the slower-migrating form (Figure 1B), demonstrating that the faster-migrating form represented oxidized Por1. When the position of one of the cysteines was shifted by

two residues, Por1 was not oxidized (Figures 1A and 1B, lanes 7–12), indicating that the oxidation assay is a sensitive means of monitoring the correct positioning of the first and last  $\beta$ -strands with respect to each other. We imported [ $^{35}$ S]Por1 into yeast mitochondria and similarly observed disulfide formation between cysteines 28 and 278 (Figure 1C). The oxidized form, but not the reduced form, was protected against protease added to the mitochondria (Figure 1C), indicating that the oxidized form was imported into mitochondria. In addition, the oxidation assay demonstrated the close proximity of the N-terminal  $\alpha$ -helix, which is located inside the porin channel, to  $\beta$ -strand 14 (Figure S1C). Taken together, these results indicate that the oxidation assay provides a means of monitoring the positioning of the first and last  $\beta$ -strands of porin with respect to each other in vivo and in organello, and thus provides evidence for formation of the  $\beta$ -barrel.

Yeast Tom40 was modeled based on the porin structure, revealing a 19-stranded  $\beta$ -barrel (Figure S1D). We generated Tom40 mutant forms containing two cysteines, one in the predicted  $\beta$ -strand 1 and one in the predicted  $\beta$ -strand 19 (Figure 1D). Because deletion of *TOM40* is lethal, we introduced the mutant forms by plasmid shuffling, and the resulting strains grew like WT yeast (Figure S1E). We analyzed nine pairwise combinations of cysteines and observed efficient oxidation only when the cysteines were directly adjacent (Figures 1D–1F), strongly supporting the modeled orientation of  $\beta$ -strands 1 and 19. Treatment with DTT shifted the faster-migrating (oxidized) form to the reduced form (Figure S1F). Modeling of the  $\beta$ -strands predicts an alternating exposure of amino acid side chains toward the pore and the lipid phase of the membrane (Figures 1D and 1F). Indeed, the sulfhydryl (SH)-reactive homobifunctional crosslinking reagent 1,4-bis(maleimido)butane (BMB), with a spacer length of 10.9 Å, efficiently crosslinked Cys87 not only to the adjacent Cys358 but also to Cys360 (both of which are predicted to face the pore side), whereas no crosslinking to Cys359 (which is predicted to face the membrane; Figure 1G) was observed. 1,1-methanediyl bismethanethiosulfonate (M1M), with a shorter spacer length (3.9 Å), efficiently crosslinked the adjacent pair Cys87 and Cys358, but not Cys87 and Cys360 (Figure 1G). We combined oxidation/reduction and crosslinking in an indirect thiol crosslinking approach: oxidant-treated mitochondria were incubated with iodoacetamide to block reduced cysteine residues, followed by DTT reduction of disulfide bonds. Crosslinking of Cys87 and Cys360, but not of Cys87 and Cys358, was inhibited (Figure S1G, crosslinker with 13 Å spacer), confirming that the adjacent residues Cys87 and Cys358 had been oxidized in mitochondria. Moreover, the oxidation assay demonstrated the predicted location of the N-terminal  $\alpha$ -helix of Tom40 inside the channel by disulfide bond formation between Cys62 and Cys200 ( $\beta$ -strand 9; Figure S1H).

We conclude that the oxidation and crosslinking assays are in full agreement with the Tom40 model (Figure 1D, S1D, and S1H). The oxidation assay provides an experimental demonstration that the  $\beta$ -barrel of Tom40 contains an odd number of  $\beta$ -strands because the position-specific disulfide bridge formation (Figures 1E and 1F) is only possible when the first and the last  $\beta$ -strands are in a parallel orientation.



(legend on next page)

### $\beta$ -Barrel Formation at the SAM Complex

To determine the import stage at which  $\beta$ -barrel formation occurred, we imported  $^{35}\text{S}$ -labeled Tom40<sub>C87/C358</sub> into isolated mitochondria. The imported Tom40 was specifically oxidized (Figure 2A) like the endogenous Tom40 (Figure 1E). To dissect the assembly pathway, we lysed mitochondria with digitonin and separated them on blue native (BN) gels. The precursor was assembled via intermediate I (SAM-bound state) and intermediate II into the mature TOM complex (Figure S2A; Model et al., 2001; Paschen et al., 2003; Wiedemann et al., 2003; Ishikawa et al., 2004; Kutik et al., 2008). We compared short and long import times to accumulate the precursors at early (SAM) and late (mature TOM) import stages. For 2D gel analysis, BN gel lanes were separated by nonreducing SDS-PAGE. After longer import times, the [ $^{35}\text{S}$ ]Tom40 precursor was observed in intermediate II and the mature TOM complex (Figure 2B, second panel). [ $^{35}\text{S}$ ]Tom40<sub>C87/C358</sub> that was assembled into the TOM complex was efficiently oxidized, as expected for the mature  $\beta$ -barrel protein. A major fraction of Tom40 that was present in intermediate II was also oxidized. After short import times, the SAM-bound state (intermediate I) as well as intermediate II were observed. Upon addition of oxidant, both reduced and oxidized Tom40 species were detected in intermediate I (Figure 2B, upper), suggesting that  $\beta$ -barrel formation may take place at the SAM complex (SAM with bound precursor migrates more slowly on BN gels compared with endogenous SAM without precursor; Paschen et al., 2003; Wiedemann et al., 2003; Stroud et al., 2011a).

To directly demonstrate that oxidation of [ $^{35}\text{S}$ ]Tom40<sub>C87/C358</sub> occurred at the SAM complex, we imported the precursor for a short time into mitochondria with Protein A-tagged Sam50 (Figure 2C). After treatment with oxidant, the mitochondria were lysed with digitonin and subjected to immunoglobulin G (IgG) affinity purification. Sam50<sub>ProtA</sub> indeed pulled down both reduced and oxidized Tom40.

Because the oxidation assay monitors the exact positioning of  $\beta$ -strands 1 and 19 with respect to each other, the generation of oxidized Tom40 provides strong evidence that the  $\beta$ -barrel has been formed. To obtain further evidence that the entire  $\beta$ -barrel was formed, we inserted cysteine pairs into several other adjacent  $\beta$ -strands. Figure S2B shows that  $\beta$ -strands 4/5 and 14/15 were in the correct position after a short-term import into mitochondria. We asked whether binding to SAM was required for  $\beta$ -barrel formation. A mutant precursor, which bound to mitochondria but not to SAM (Leu357 and Phe359 of the  $\beta$ -signal replaced by Gln; Kutik et al., 2008), was not

oxidized (Figure S2C). Additionally, we asked whether accumulation at SAM was sufficient for oxidation of a mutant precursor without formation of the correct  $\beta$ -barrel. We generated a Tom40<sub>C87/C358</sub> precursor, which lacked several  $\beta$ -strands but efficiently accumulated at SAM (Int-I; Figure S2D). As expected, no oxidation of the mutant precursor was observed.

Taken together, these results show that the position-specific oxidation assay monitors the formation of the Tom40  $\beta$ -barrel in organello, and demonstrate that the full  $\beta$ -barrel with correct positioning of the first and last  $\beta$ -strands is formed in the SAM-bound state.

Where is the  $\beta$ -barrel inserted into the lipid phase of the outer membrane? Treatment of mitochondria at alkaline pH has been used to analyze membrane integration of proteins, because soluble and peripheral membrane proteins are extracted (Thornton et al., 2010). Previous studies suggested that  $\beta$ -barrel precursors bound to SAM (intermediate I) are not inserted into the lipid phase of the outer membrane because alkaline treatment dissociated the intermediate I when analyzed on BN gels (Model et al., 2001; Kutik et al., 2008). However, this approach did not differentiate between the alkaline resistance of SAM itself and that of the bound precursor. Whereas the TOM complex including the fully assembled [ $^{35}\text{S}$ ]Tom40 was shown to be resistant to alkaline extraction, the SAM complex was dissociated when analyzed by BN electrophoresis (Figure S2E; Meisinger et al., 2001; Kutik et al., 2008) (TOM contains only integral membrane proteins, whereas SAM includes peripheral membrane proteins). We used a mutant form of Tom40 in which replacement of Gly354 by Ala led to an arrest of the precursor at SAM (Kutik et al., 2008). Like the WT precursor, this precursor was resistant to alkaline extraction (Figure 2D). For comparison, a mutant precursor that bound to mitochondria but not to SAM (Phe359 replaced by Gln; Kutik et al., 2008) was extracted at alkaline pH, demonstrating that it was not integrated into the membrane. We conclude that a  $\beta$ -barrel precursor becomes membrane integrated in the SAM-bound state, whereas a precursor that cannot bind to SAM is not membrane integrated.

### Involvement of the Import Receptor Tom22 in $\beta$ -Barrel Formation

We employed the oxidation assay to define components required for  $\beta$ -barrel folding. We first used mutant mitochondria with defects of SAM, a deletion mutant of Sam37, and conditional mutants of the essential components Sam35 and Sam50. The formation of oxidized Tom40 was strongly impaired

#### Figure 1. Disulfide Monitoring of $\beta$ -Barrel Formation in Mitochondria

- (A) Scheme of *Saccharomyces cerevisiae* Por1 (upper) and its  $\beta$ -barrel (left). Por1 homology model with disulfide bond (red) between cysteines 28/278 (right).  
 (B) Mitochondria from yeast strains expressing Por1 variants were treated with 4-DPS (lanes 2, 5, 8, and 11) or CuSO<sub>4</sub> (lanes 3, 6, 9, 12, 14, and 15) followed by DTT (lane 15), and analyzed by nonreducing SDS-PAGE, western blotting, and immunodetection.  
 (C) [ $^{35}\text{S}$ ]Por1<sub>C28/C278</sub> was imported into WT mitochondria followed by proteinase K treatment, oxidation with CuSO<sub>4</sub>, nonreducing SDS-PAGE, and autoradiography.  
 (D) Schemes of yeast Tom40 as in (A). Homology model of the Tom40  $\beta$ -barrel structure with disulfide bonds (orange/red) between residues 87/358, 88/359, and 89/360.  
 (E) Mitochondria from yeast strains expressing Tom40 variants were treated with the oxidant CuP and subjected to immunodetection as in (B).  
 (F) Summary of disulfide bond formation (+) and failed oxidation (–) of Tom40 variants.  
 (G) Mitochondria from yeast strains expressing Tom40 variants were treated with BMB or M1M and analyzed by SDS-PAGE and immunodetection.  
 See also Figure S1.

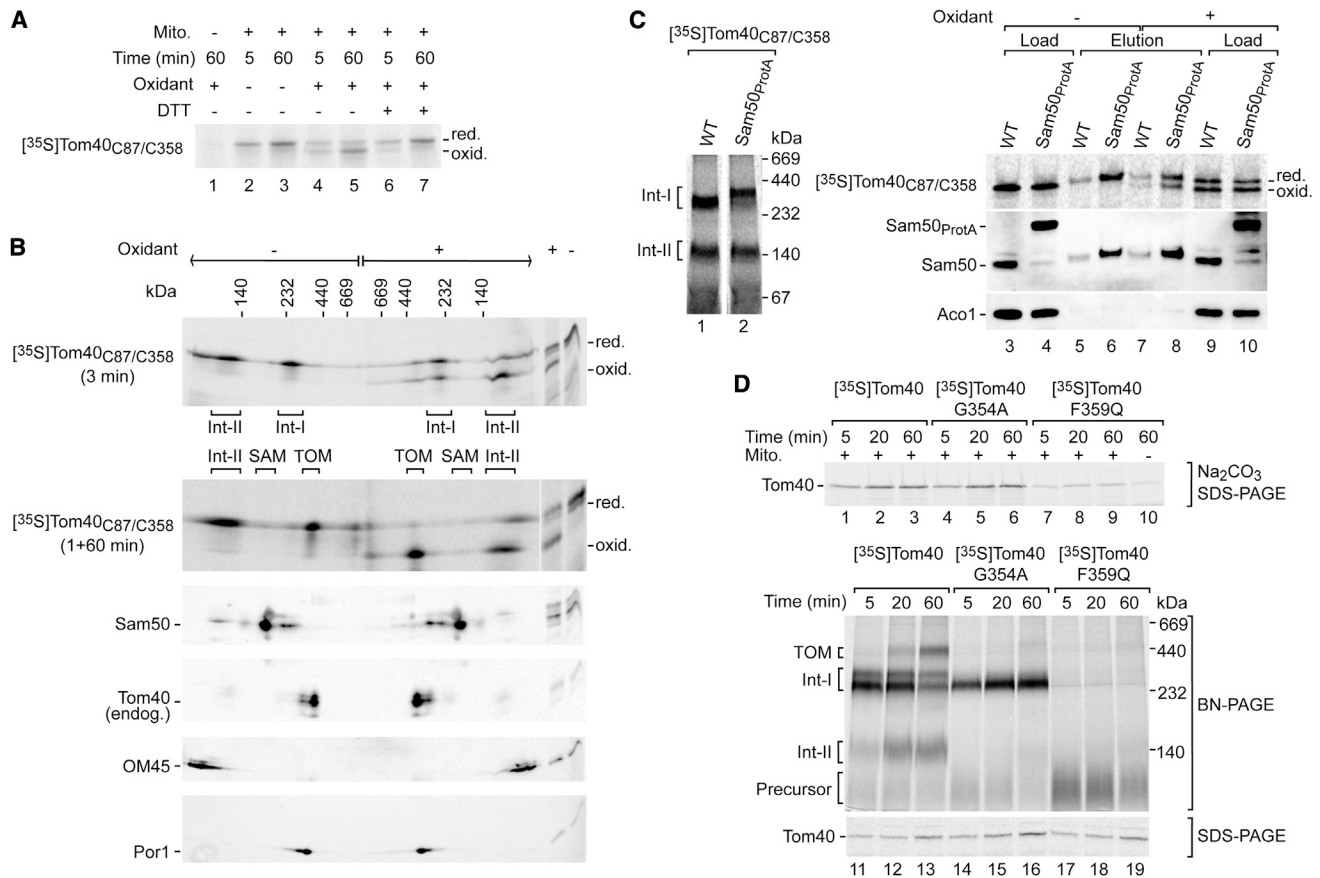


**Figure 2.  $\beta$ -Barrel Formation by the SAM-Bound Precursor**

(A) [<sup>35</sup>S]Tom40<sub>C87/C358</sub> was imported into WT mitochondria followed by CuP or DTT treatment (as indicated), nonreducing SDS-PAGE, and autoradiography. (B) [<sup>35</sup>S]Tom40<sub>C87/C358</sub> was imported into WT mitochondria for 3 min or 1 + 60 min (chase). After CuP treatment, samples were subjected to BN plus second-dimension nonreducing SDS-PAGE and analyzed by autoradiography or immunodetection. (C) [<sup>35</sup>S]Tom40<sub>C87/C358</sub> was imported for 3 min into WT and Sam50<sup>ProtA</sup> mitochondria. Left: BN-PAGE. Right: after oxidation with CuP, mitochondria were lysed and subjected to IgG-Sepharose purification and nonreducing SDS-PAGE. Load: 4%; elution: 100%. (D) [<sup>35</sup>S]Tom40 precursors were imported into WT mitochondria and analyzed by BN-PAGE or SDS-PAGE (middle and lower). The pellet after carbonate extraction was analyzed by SDS-PAGE (upper). See also Figure S2.

in the mutants (Figure 3A), as expected for the role of SAM in  $\beta$ -barrel formation.

We then analyzed the two initial import receptors, Tom20 and Tom70. The overall import efficiency of Tom40 was reduced in *tom20* $\Delta$  and *tom70* $\Delta$  mutant mitochondria, as expected; however, imported Tom40 was still converted to the oxidized form with good efficiency (Figure 3B). The ratio of oxidized to reduced Tom40 was only mildly affected in the mutant mitochondria (Figure 3E), indicating that Tom20 and Tom70 are not crucial for  $\beta$ -barrel formation at SAM.

With mutants of the three small Tom proteins, we observed a differential result. Mitochondria lacking Tom6 or Tom7 formed oxidized Tom40 with an efficiency close to that of WT mitochondria (Figures 3C and 3E). However, *tom5* $\Delta$  mitochondria showed a strong inhibition of Tom40 oxidation. This finding fits with a report by Becker et al. (2010) that Tom5 has a dual localization: although Tom5 is located in TOM, a fraction of Tom5

molecules are also part of SAM and are directly transferred to the SAM-bound Tom40 precursor. Thus, Tom5 promotes the folding of Tom40 at the SAM complex.

Unexpectedly, mitochondria lacking the central receptor Tom22 were considerably impaired in Tom40 oxidation (Figures 3D and 3E). Similarly, oxidation of imported Por1<sub>C28/C278</sub> was inhibited in *tom22* $\Delta$  mitochondria (Figure S3A). Tom22 thus exerts a significant influence on  $\beta$ -barrel folding, raising the possibility that Tom22 may be connected to SAM. Initial studies on the SAM pathway indicated that translocation of  $\beta$ -barrel precursors through TOM to a protease-protected location was partially impaired in SAM mutants, suggesting that TOM translocation and precursor recognition by SAM may be directly or indirectly coupled (Paschen et al., 2003; Wiedemann et al., 2003; Ishikawa et al., 2004; Habib et al., 2007). However, because no mechanistic explanation was demonstrated, current models on the  $\beta$ -barrel pathway depict TOM and SAM as

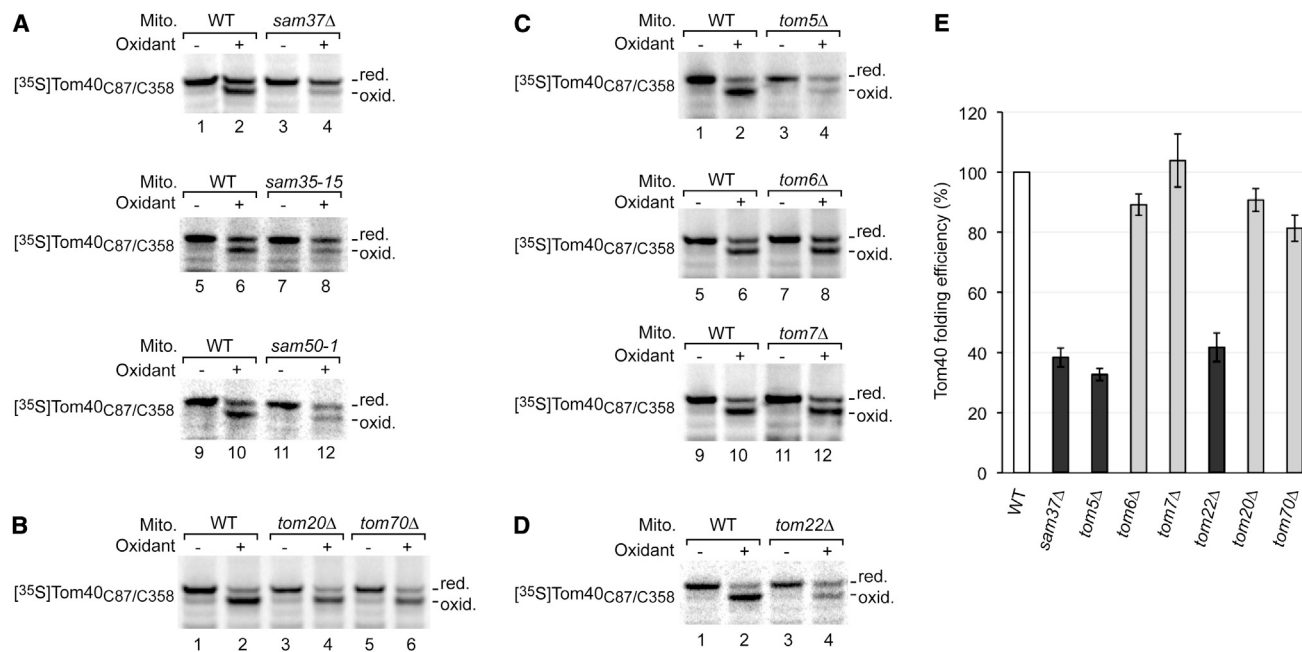


**Figure 3.  $\beta$ -Barrel Formation Is Inhibited in Mitochondria Lacking Tom22**

(A)–(D) [ $^{35}\text{S}$ ]Tom40<sub>C87/C358</sub> was imported into the indicated mitochondria for 5 min, followed by oxidation with CuP, nonreducing SDS-PAGE, and autoradiography.

(E) Quantification of the folding efficiency (ratio of oxidized over reduced Tom40; mean  $\pm$  SEM;  $n \geq 3$ ) from experiments corresponding to (A)–(D). WT was set to 100%.

See also Figure S3.

independent machineries (Neupert and Herrmann, 2007; Becker et al., 2009; Endo and Yamano, 2010; Schmidt et al., 2010; Dukanovic and Rapaport, 2011; Hewitt et al., 2011; Klein et al., 2012; Shiota et al., 2012). We used two approaches to study a possible involvement of SAM in translocation of the Tom40 precursor to a protease-protected location. Mitochondria lacking Sam37 were indeed partially impaired in import of Tom40 (Figure S3B). Similarly, a mutant Tom40 precursor, which was impaired in binding to SAM due to a defective  $\beta$ -signal (Phe359 replaced by Gln; Kutik et al., 2008), was impaired in translocation to a protease-protected location (Figure S3C). Together with the inhibition of  $\beta$ -barrel folding in *tom22Δ* mitochondria, the protease protection assays support the view that SAM and TOM may be connected to each other by an unknown mechanism.

#### Identification of a TOM-SAM Supercomplex

To test for a possible interaction of TOM and SAM, we used stable isotope labeling with amino acids in cell culture (SILAC) and quantitative mass spectrometry. WT yeast cells were grown in the presence of the heavy amino acids [ $^{13}\text{C}/^{15}\text{N}$ ]Arg and [ $^{13}\text{C}/^{15}\text{N}$ ]Lys, whereas Sam50<sub>ProTA</sub> cells were grown on standard (light) amino acids. Upon lysis of cell extracts with digitonin, the SAM complex was purified by affinity chromatography, and heavy and light samples were mixed and analyzed by mass spectrometry. Light/heavy ratios for the identified peptides demonstrated a specific copurification of all SAM subunits, as well as subunits of the mitochondrial inner membrane organizing system (MINOS), as expected (Figure 4A; Table S1; Harner et al.,

2011; Bohnert et al., 2012). In addition, Tom40, Tom22, and Tom20 were specifically enriched with light/heavy ratios, similar to what was observed for the SAM subunits. Thus, quantitative mass spectrometry revealed copurification of three major TOM subunits with SAM.

To directly test whether TOM and SAM were associated, we performed pull-down experiments from yeast strains containing tagged Sam50 or tagged Tom22. Sam50<sub>ProTA</sub> pulled down not only SAM subunits but also a fraction of TOM subunits (Figure 4B). Similarly, Tom22<sub>His</sub> pulled down TOM subunits and a fraction of SAM subunits (Figure 4C). Various control proteins were not copurified with SAM or TOM. These results indicate that a fraction of TOM and SAM complexes interact with each other.

However, up to now, a putative TOM-SAM supercomplex has not been observed by BN electrophoresis. We optimized the protein/detergent ratio to diminish the dissociation of labile complexes during electrophoretic separation. Eluates of isolated SAM complexes were analyzed by BN electrophoresis and immunodecoration with antibodies against Tom40 and Tom22. In addition to copurified TOM complexes, a larger complex of  $\sim 650$  kDa was detected (Figure 4D). Direct BN analysis of lysed mitochondria and decoration with antibodies against Sam50 revealed the known SAM<sub>core</sub> and SAM-Mdm10 complexes, but also the 650 kDa complex (Figure 4E). Importantly, in mutant mitochondria lacking either Sam37 or Tom22, the large complex was not observed (Figure 4E). In mutant mitochondria lacking Tom5, Tom20, or Tom70, pull-down of TOM subunits with tagged

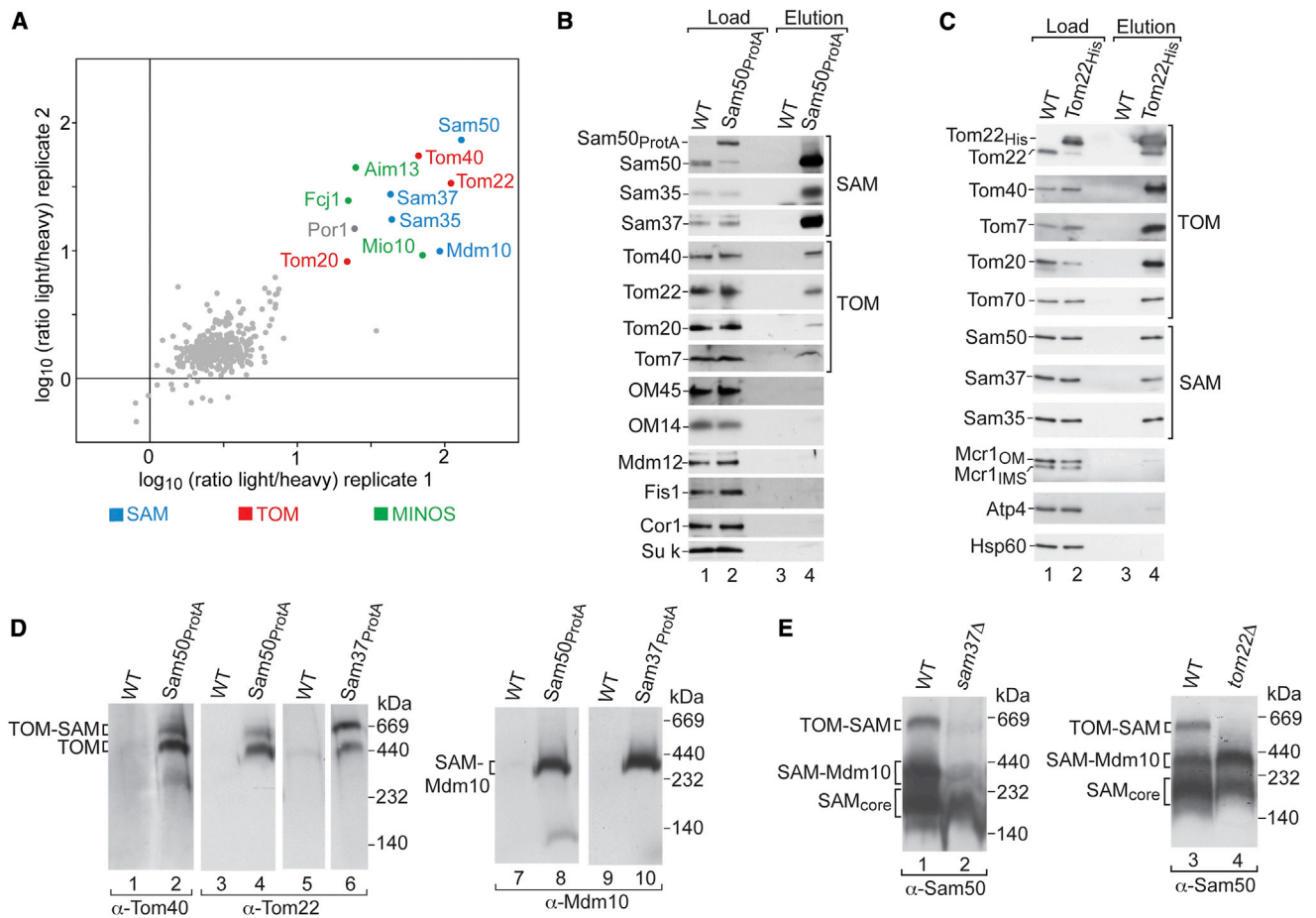


**Figure 4. TOM and SAM Form a Supercomplex**

(A) Sam50<sup>ProTA</sup> yeast strain was grown on standard (light) amino acids and WT yeast in the presence of [<sup>13</sup>C/<sup>15</sup>N]Arg/Lys (heavy). IgG purification of cell extracts was quantified via mass spectrometry. Significantly enriched proteins are annotated.

(B) Yeast cell extracts of WT or Sam50<sup>ProTA</sup> strain were subjected to IgG purification and analyzed by SDS-PAGE and immunodecoration. Load: 0.5%; elution: 100%.

(C) Proteins isolated from WT and Tom22<sup>His</sup> mitochondria by Ni-NTA were detected as in (B). Load: 3%; elution: 100%.

(D) Eluates of IgG purified cell extracts of WT, Sam50<sup>ProTA</sup>, and Sam37<sup>ProTA</sup> yeast were subjected to BN-PAGE and immunodecoration.

(E) WT, *sam37Δ*, and *tom22Δ* mitochondria were analyzed by BN-PAGE and immunodecoration.

See also Table S1 and Figure S4.

Sam37 and detection of the TOM-SAM supercomplex were not blocked (Figures S4A and S4B), indicating that these Tom proteins are not crucial for TOM-SAM interaction.

Taken together, the SILAC analysis, pulldown experiments, and BN electrophoresis indicate that a fraction of TOM and SAM complexes are associated in a supercomplex of ~650 kDa. The TOM-SAM supercomplex is labile upon lysis of mitochondria, providing an explanation as to why it escaped detection in previous studies. Although the three SAM<sub>core</sub> subunits (Sam50, Sam37, and Sam35) were copurified with TOM, Mdm10 was not found in the supercomplex. Mdm10-antibodies decorated the SAM-Mdm10 complex, but not the supercomplex (Figure 4D). This fits with the apparent BN mobility of the supercomplex of ~650 kDa, which indicates that one TOM complex (~450 kDa) and one SAM<sub>core</sub> complex (~200 kDa) are associated in the supercomplex.

### Small TIM Chaperones Interact with the TOM-SAM-Preprotein Supercomplex

When protein synthesis was stopped by addition of cycloheximide to yeast cells, formation of the TOM-SAM supercomplex was not blocked (Figure S5A), indicating that ongoing protein synthesis is not essential for supercomplex formation. Because the supercomplex is labile, however, we searched for an artificial tether to stabilize it. Fusion proteins have been used to stabilize the TOM-TIM23 supercomplex (Chacinska et al., 2003; Figure 5A, lane 2). We tested a fusion protein between an N-terminal portion of cytochrome *b*<sub>2</sub> and Tom40 (Shiota et al., 2012). Upon incubation with mitochondria in the absence of an inner membrane potential, *b*<sub>2</sub>(220)-Tom40 was accumulated in a complex of ~700 kDa (Figure 5A). Since the size of the complex fits with a TOM-SAM supercomplex plus arrested fusion protein, we performed pulldown experiments followed by BN analysis. Arrested

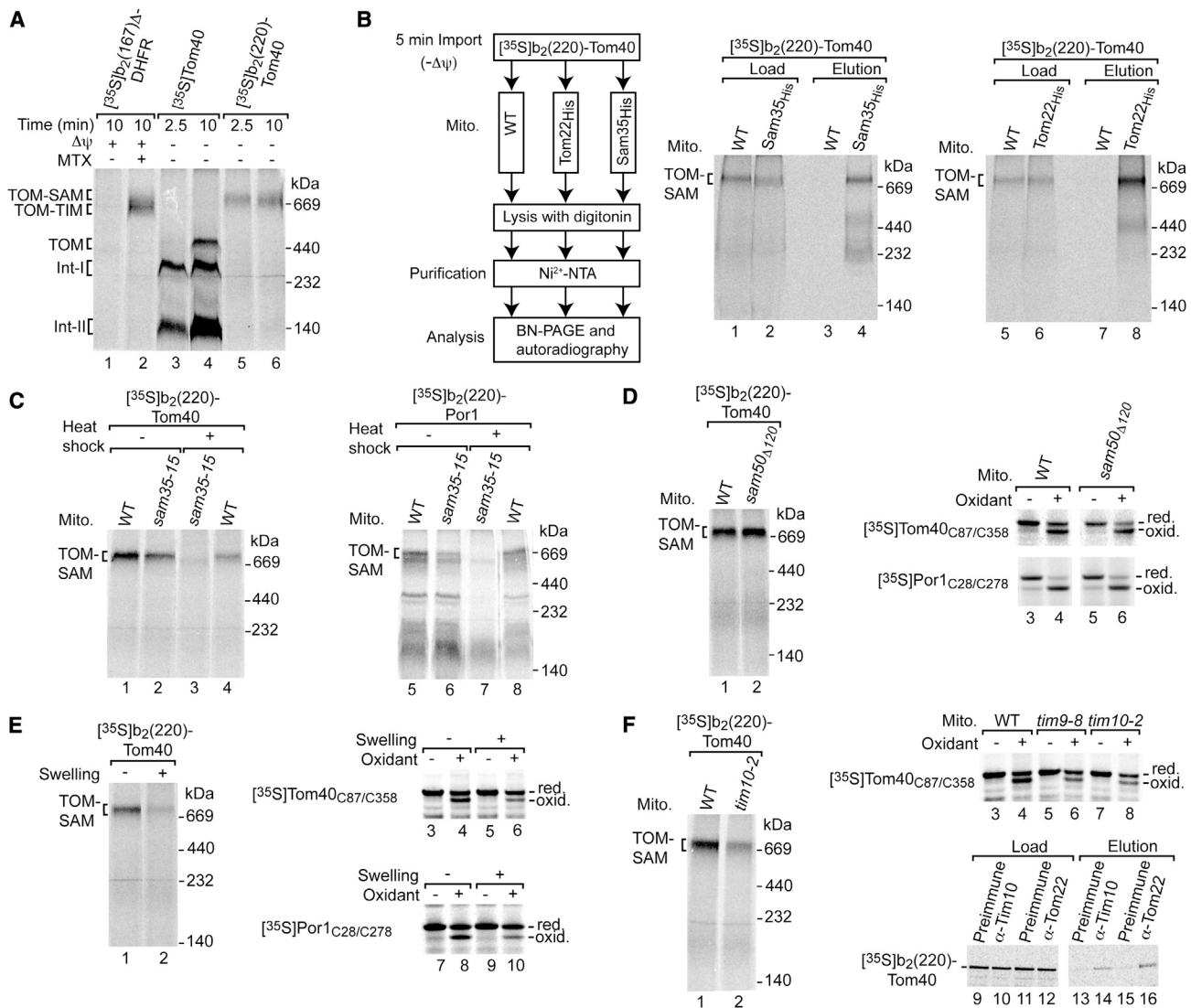


**Figure 5. TOM-SAM-Preprotein Supercomplex Interacts with Small TIM Chaperones**

(A) [<sup>35</sup>S]precursors were imported into WT mitochondria and analyzed by BN-PAGE and autoradiography. Δψ, membrane potential; MTX, methotrexate. (B) [<sup>35</sup>S]b<sub>2</sub>(220)-Tom40 was imported into mitochondria, followed by Ni-NTA purification and analysis as in (A). Load: 7%; elution: 100%. (C) Where indicated, WT and *sam35-15* mitochondria were incubated at 37°C for 15 min before [<sup>35</sup>S]precursors were imported and analyzed as in (A). (D) [<sup>35</sup>S]b<sub>2</sub>(220)-Tom40 was imported for 5 min into the indicated mitochondria, followed by BN-PAGE (left). [<sup>35</sup>S]Tom40<sub>C87/C358</sub> was imported for 5 min, treated with CuP, and analyzed by nonreducing SDS-PAGE (upper right). [<sup>35</sup>S]Por1<sub>C28/C278</sub> was imported, and mitochondria were treated with proteinase K and subsequently CuSO<sub>4</sub> (lower-right). (E) b<sub>2</sub>(220)-Tom40, Tom40, and Por1 precursors were imported into mitochondria or mitoplasts (+ swelling) and analyzed as in (D) (without proteinase K treatment). (F) Left: import into WT and *tim10-2* mitochondria as in (D). Upper-right: import into mitochondria after heat shock as in (D). Lower: [<sup>35</sup>S]b<sub>2</sub>(220)-Tom40 was imported into WT mitochondria for 5 min, followed by immunoprecipitation. Load: 3%; elution: 100%. See also Figure S5.

b<sub>2</sub>(220)-Tom40, as well as a comparable b<sub>2</sub>(220)-Por1 fusion protein, was indeed copurified with tagged Sam35 and tagged Tom22, and the 700 kDa complex remained stable (Figures 5B and S5B), demonstrating that the fusion proteins were associated with both TOM and SAM. Antibodies against cytochrome b<sub>2</sub> added to intact mitochondria quantitatively shifted the TOM-SAM-preprotein complex (Figure S5C), indicating that

(part of) the N-terminal b<sub>2</sub> portion was located on the mitochondrial surface. Accumulated b<sub>2</sub>(220)-Tom40 was extracted at alkaline pH, whereas Tom40 itself was further transported to a carbonate-resistant location as expected (Figure S5D). To probe whether generation of the TOM-SAM-preprotein complex required a functional SAM complex, we made use of the temperature-sensitive *sam35-15* mutant (Kutik et al., 2008).

Accumulation of  $b_2(220)$ -Tom40 and  $b_2(220)$ -Por1 in the TOM-SAM supercomplex was blocked in the mutant mitochondria upon heat treatment (Figure 5C). Thus, a single polypeptide chain simultaneously interacts with TOM and SAM, leading to the formation of a stable TOM-SAM-preprotein supercomplex.

The N-terminal polypeptide transport-associated (POTRA) domain of Sam50 is not required for binding of  $\beta$ -barrel precursors to SAM, but is involved in the subsequent release of proteins from SAM (Kutik et al., 2008; Stroud et al., 2011a). Generation of the TOM-SAM-preprotein supercomplex was not impaired in mitochondria lacking the Sam50 POTRA domain (Figure 5D). Similarly, oxidation (folding) of Tom40<sub>C87/C358</sub> and Por1<sub>C28/C278</sub> occurred with WT efficiency in the mutant mitochondria, demonstrating that supercomplex formation and  $\beta$ -barrel folding occur before the POTRA-dependent step.

Small TIM chaperones of the intermembrane space are involved in the biogenesis of  $\beta$ -barrel proteins (Hoppins and Nargang, 2004; Wiedemann et al., 2004). We asked whether accumulation of the  $b_2(220)$ -Tom40 fusion protein in the TOM-SAM supercomplex depended on intermembrane space components. Upon swelling of mitochondria to rupture the outer membrane and release intermembrane space proteins (Figure S5E), accumulation of the fusion protein in the supercomplex was inhibited (Figure 5E). Similarly, the oxidation assay revealed a dependence on an intact intermembrane space for formation of the  $\beta$ -barrels of Tom40 and Por1 (Figure 5E). Conditional mutants of the small TIM chaperones impaired formation of the TOM-SAM-preprotein supercomplex and oxidation (folding) of Tom40<sub>C87/C358</sub> (Figure 5F). To directly test whether arrested  $b_2(220)$ -Tom40 interacted with small TIM chaperones, we used coimmunoprecipitation. Antibodies directed against Tim10 specifically copurified the arrested fusion protein (Figure 5F, lane 14). We conclude that small TIM chaperones interact with the TOM-SAM-preprotein supercomplex and promote  $\beta$ -barrel formation.

### Tom22 Connects TOM and SAM Complexes

Since Tom22 promotes  $\beta$ -barrel folding at SAM, we asked whether Tom22 plays a direct role in formation of the TOM-SAM supercomplex. Mitochondria lacking Tom22 were blocked in formation of the TOM-SAM-preprotein supercomplex (Figure 6A). Because mitochondria lacking Tom22 are defective in most mitochondrial protein import pathways (van Wilpe et al., 1999), we asked whether Tom22 directly or indirectly affected  $\beta$ -barrel biogenesis. First, we found that chemical amounts of Tom22 imported into *tom22* $\Delta$  mitochondria stimulated the import and assembly of Tom40 (Figure S6A) and formation of the TOM-SAM-preprotein supercomplex (Figure 6A, lane 3), demonstrating that Tom22 itself rescued the mutant. We then generated *tom22* yeast mutants and selected the mutant strain *tom22-102* that showed a selective import defect. The mutant mitochondria were strongly impaired in  $\beta$ -barrel biogenesis, but only mildly affected in presequence and carrier pathways to the inner membrane (Figures 6B and S6B) (the levels of TOM and SAM proteins were only moderately affected; Figure S6C). Formation of the TOM-SAM-preprotein supercomplex was blocked in *tom22-102* mitochondria (Figure 6C). To exclude the possibility that SAM was inactive in this strain, we analyzed

binding of a purified  $\beta$ -signal (fused to glutathione S transferase) to SAM (Kutik et al., 2008). The  $\beta$ -signal efficiently pulled down the SAM complex of WT and *tom22-102* mitochondria (Figure 6C). The binding was specific, as inactivation of the  $\beta$ -signal by a single amino acid replacement inhibited binding to SAM. The analysis of the *tom22-102* mutant indicates that Tom22 plays a selective role in  $\beta$ -barrel import that can be separated from its role in the presequence and carrier import pathways. Finally, to probe whether Tom22 was in physical proximity to SAM, we added the crosslinking reagent disuccinimidyl glutarate (DSG) to mitochondria containing tagged Tom22. A crosslinking product of  $\sim 75$  kDa was generated that was purified with tagged Tom22 under denaturing conditions and reacted with antibodies against Sam50 (Figure 6D), demonstrating that it represented a Tom22-Sam50 crosslinking product. Neither tagged Tom20 nor tagged Tom70 pulled down a Sam50 crosslinking product.

Taken together with the oxidation (folding) assay, these results indicate that Tom22 plays a specific role in the folding pathway of  $\beta$ -barrel proteins. Tom22 interacts with the SAM complex and thus promotes formation of the TOM-SAM supercomplex.

Tom22 exposes an N-terminal receptor domain to the cytosol and a C-terminal domain to the intermembrane space (van Wilpe et al., 1999; Dolezal et al., 2006; Neupert and Herrmann, 2007; Yamano et al., 2008). We asked which domain was involved in formation of the TOM-SAM supercomplex. *tom22* <sub>$\Delta$ IMS</sub> mitochondria lacking the entire intermembrane space domain efficiently formed the TOM-SAM-preprotein supercomplex, and  $\beta$ -barrel formation occurred with WT efficiency (Figure 6E). Thus, the intermembrane space domain of Tom22 is not required for supercomplex formation or  $\beta$ -barrel folding.

To study a potential role of the Tom22 receptor domain in the TOM-SAM supercomplex, we bound the purified and His-tagged receptor domain to a nickel-nitrilotriacetic acid (Ni-NTA) column and performed affinity purification from lysed mitochondria. SAM subunits were specifically copurified with the cytosolic domain of Tom22, but not control proteins including the abundant porin (Figure 6F). For comparison, none of the SAM subunits was copurified with the cytosolic domains of Tom20 and Tom70. We constructed a yeast strain in which Tom22 contained a single cysteine in its cytosolic domain. The SH-specific crosslinking reagent bis(maleimido)ethane (BMOE; 8 Å spacer) generated Tom22-Sam50 crosslinking products (Figure 6G). We conclude that the cytosolic receptor domain of Tom22 interacts with SAM and thus promotes the generation of a TOM-SAM supercomplex.

### DISCUSSION

We developed an assay to analyze mitochondrial  $\beta$ -barrel folding in the native environment, and demonstrated that the Tom40  $\beta$ -barrel is formed and inserted into the outer membrane while the precursor is bound to the SAM complex. The exact positioning of the first and last  $\beta$ -strands, as well as internal pairs of  $\beta$ -strands, was monitored by position-specific disulfide formation (oxidation). The folding (oxidation) assay enabled us to define factors required for  $\beta$ -barrel formation in intact mitochondria. We observed an unexpected connection between TOM

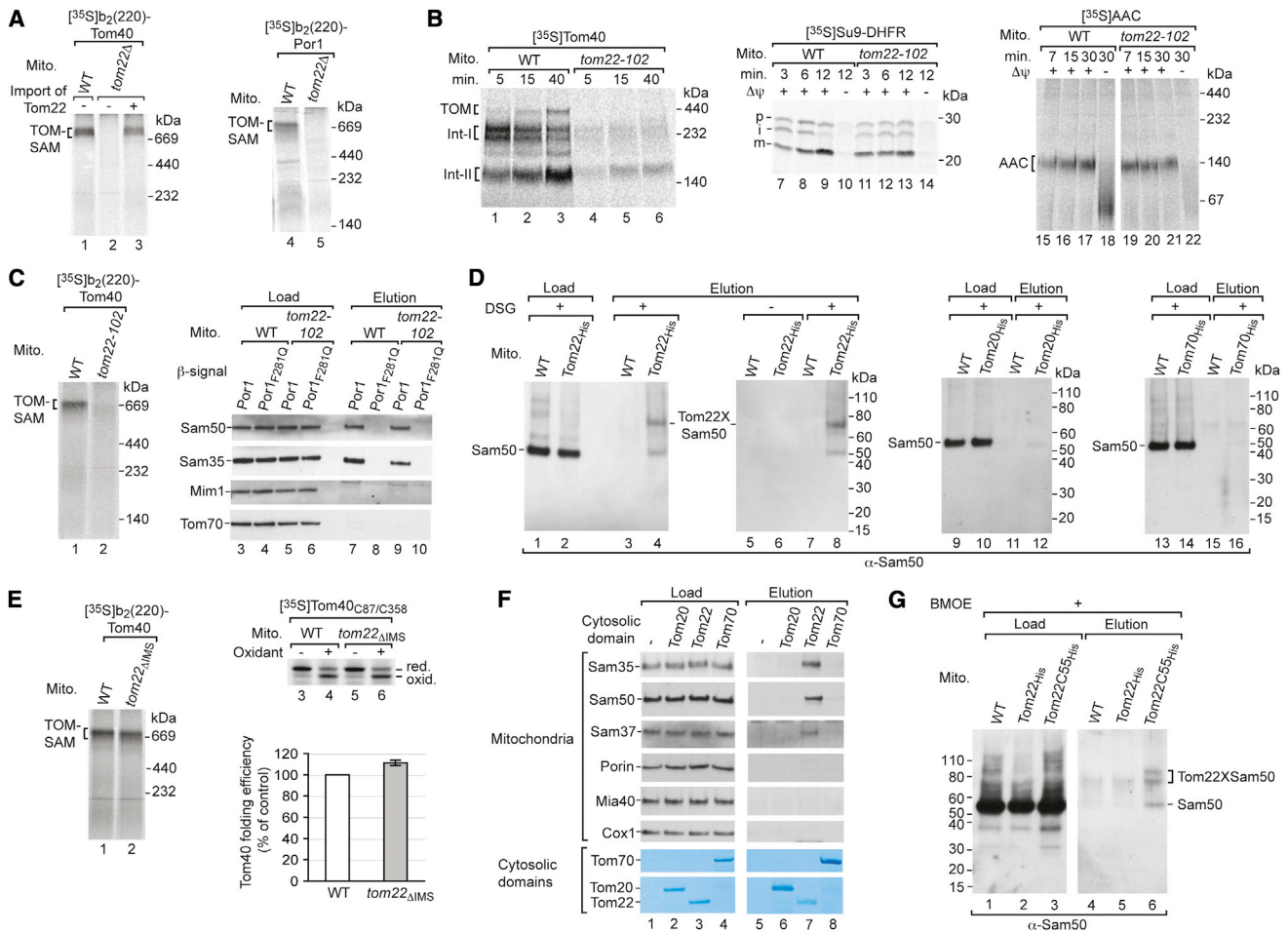


**Figure 6. The Receptor Domain of Tom22 Links TOM and SAM**

(A) WT and *tom22* $\Delta$  mitochondria were incubated with or without chemical amounts of Tom22. Subsequently, [<sup>35</sup>S]precursors were imported ( $-\Delta\psi$ ) and analyzed by BN-PAGE and autoradiography.

(B) [<sup>35</sup>S]precursors were imported into isolated WT or *tom22-102* mitochondria and subjected to BN- or SDS-PAGE.

(C) Left: [<sup>35</sup>S]b<sub>2</sub>(220)-Tom40 was imported into WT and *tom22-102* mitochondria as in (A). Right: digitonin-lysed WT and *tom22-102* mitochondria were incubated with Por1  $\beta$ -signal (WT or F281Q) fused to glutathione S transferase and bound to glutathione-Sepharose beads. Load (25%) and elution (100%) fractions were subjected to SDS-PAGE and immunodecoration.

(D) WT, Tom22<sup>His</sup>, Tom20<sup>His</sup>, and Tom70<sup>His</sup> mitochondria were treated with DSG, lysed with SDS, and subjected to affinity purification via Ni-NTA. Load (3%, lanes 1 and 2; 0.5%, lanes 9, 10, 13 and 14) and elution (100%) fractions were analyzed by SDS-PAGE and immunodecoration.

(E) Import into WT and *tom22* $\Delta$ IMS mitochondria as in Figure 5D. The folding efficiency (mean  $\pm$  SEM; n = 4) was determined as in Figure 3E.

(F) Ni-NTA agarose beads coated with the cytosolic domains of Tom20, Tom22, and Tom70 were incubated with digitonin-lysed WT mitochondria and washed. Load (0.5%) and elution of mitochondria (100%) were analyzed by SDS-PAGE and immunodecoration. Load (7.5%) and elution (30%) of cytosolic domains were analyzed by SDS-PAGE and Coomassie staining.

(G) WT, Tom22<sup>His</sup>, and Tom22C55<sup>His</sup> mitochondria were treated with BMOE, lysed with SDS, and subjected to Ni-NTA purification. Load (0.5%) and elution fractions (100%) were analyzed by SDS-PAGE and immunodecoration.

See also Figure S6.

and SAM complexes via the receptor Tom22. The folding assay separated the analysis of  $\beta$ -barrel formation from precursor import through the TOM complex. Although mutants lacking the receptors Tom20 or Tom70 decreased the import efficiency of  $\beta$ -barrel precursors as expected (Rapaport and Neupert, 1999; Krimmer et al., 2001; Model et al., 2001; Yamano et al., 2008), they did not alter the folding efficiency of the imported proteins. Mutant mitochondria lacking Tom22, however, not only imported the precursors with reduced efficiency (Krimmer

et al., 2001; Model et al., 2001; Yamano et al., 2008) but were also strongly impaired in  $\beta$ -barrel folding. Up to now, TOM and SAM complexes have been considered as independent machineries (Neupert and Herrmann, 2007; Endo and Yamano, 2010; Schmidt et al., 2010; Dukanovic and Rapaport, 2011; Hewitt et al., 2011; Klein et al., 2012; Shiota et al., 2012). We report a new function for Tom22. The central TOM import receptor directly interacts with SAM via its cytosolic receptor domain. Thus, Tom22 connects the two translocases into a

supercomplex of ~650 kDa, consisting of one TOM complex and one SAM complex.

TOM is the main protein entry gate of mitochondria, and thus far, four import pathways are known that use the TOM import channel: the presequence pathway, carrier pathway, intermembrane space pathway, and  $\beta$ -barrel pathway (Neupert and Herrmann, 2007; Schmidt et al., 2010; Hewitt et al., 2011). TOM complexes are ~3-fold more abundant than the presequence translocase (TIM23 complex) and ~4-fold more abundant than SAM complexes (Ghaemmaghani et al., 2003), which explains how TOM can feed precursor proteins into different downstream machineries. Our results indicate that a fraction of TOM and SAM complexes associate in a supercomplex in the absence of added  $\beta$ -barrel precursors. We constructed an artificial tether, a fusion protein that was accumulated in both TOM and SAM, to stabilize the TOM-SAM supercomplex. The functional requirements for accumulation of this fusion protein in the supercomplex agreed well with the requirements for  $\beta$ -barrel formation in the folding (oxidation) assay. In particular, a dependence on the small TIM chaperones (Hoppins and Nargang, 2004; Wiedemann et al., 2004) was observed under both assay conditions. Thus, elements on both sides of the outer membrane promote  $\beta$ -barrel biogenesis. The cytosolic receptor domain of Tom22 connects TOM and SAM, and the small TIM chaperones help in precursor transfer on the intermembrane space side.

The initial finding that  $\beta$ -barrel precursors are first translocated across the outer membrane to the intermembrane space side (Model et al., 2001; Wiedemann et al., 2003, 2004; Hoppins and Nargang, 2004) prompted the development of various models to explain the mechanisms of precursor transfer from TOM to SAM. On the one hand, it was speculated that  $\beta$ -barrel precursors may form soluble intermediates in the intermembrane space before being exported into the outer membrane (Neupert and Herrmann, 2007; Becker et al., 2009; Tommassen, 2010; Dukanovic and Rapaport, 2011). Despite a large number of studies on the  $\beta$ -barrel pathway, however, a soluble intermediate in the intermembrane space has not been found. On the other hand, a possible coupling of precursor translocation through TOM and recognition by SAM was discussed (Paschen et al., 2003; Ishikawa et al., 2004; Habib et al., 2007; Walther et al., 2009). However, no molecular mechanism was found, because all models were based on the assumption that TOM and SAM were separate, noninteracting machineries (Neupert and Herrmann, 2007; Becker et al., 2009; Walther et al., 2009; Endo and Yamano, 2010; Schmidt et al., 2010; Dukanovic and Rapaport, 2011; Hewitt et al., 2011; Klein et al., 2012; Shiota et al., 2012). The identification of the TOM-SAM supercomplex suggests an efficient substrate transfer from TOM to SAM. The translocases are in physical contact and a single precursor polypeptide can span both translocases simultaneously. Thus, there is no need for a soluble intermediate, but the small TIM chaperones interact with the preprotein that has accumulated in TOM and SAM and support precursor transfer, likely by shielding hydrophobic regions of the precursors exposed to the intermembrane space. We propose that formation of the TOM-SAM supercomplex promotes substrate channeling in the  $\beta$ -barrel pathway. Indeed,  $\beta$ -barrel formation is considerably more effi-

cient when Tom22 is present, i.e., when the TOM-SAM supercomplex can be formed.

In summary, folding and membrane insertion of mitochondrial  $\beta$ -barrel proteins occur in the SAM-bound state, and this has interesting implications for the bacterial BAM complex (Tomassen, 2010; Hagan et al., 2011). In addition, mitochondria have evolved an efficient system to integrate the complicated translocation pathways of  $\beta$ -barrel precursors that have to be transported across the outer membrane in both directions. Receptor-mediated coupling of import and export translocases into a supercomplex provides a novel and efficient means of precursor transfer (substrate channeling).

## EXPERIMENTAL PROCEDURES

### Generation of Site-Specific Cysteine Mutants of Tom40, Porin, and Tom22

We generated Tom40 and Por1 constructs using pFL39 plasmids encoding the WT forms as a template. The endogenous cysteines of Tom40 (C165W, C326A, C341S, and C355F) or Por1 (C130D and C210S) were replaced by QuikChange PCR (Stratagene). Subsequently, cysteine residues were introduced at specific sites. pFL39-Tom22<sub>His</sub> was generated based on pFL39-Tom22 and used as a template to generate pFL39-Tom22C55<sub>His</sub>. These constructs were used to generate yeast strains expressing Tom40, Por1, or Tom22 cysteine mutants. pFL39 encoding WT or cysteine mutants of TOM40 was transformed into a YPH499 *tom40* $\Delta$  strain containing a YEp352 plasmid encoding WT TOM40 and a URA3 marker (2547) (Kutik et al., 2008). pFL39 encoding WT, His-tagged WT, or the cysteine mutant of TOM22 was transformed into a YPH499 *tom22* $\Delta$  strain containing pYEp352-TOM22 (2281). Loss of pYEp352-TOM40 or pYEp352-TOM22 was monitored by growth on 5-fluoroorotic acid medium. Plasmids encoding pFL39-POR1 or POR1 mutants were transformed into the yeast strain *por1* $\Delta$ , followed by selection on selective medium lacking tryptophan (Stroud et al., 2011a).

### In Vitro Import Assays, BN Electrophoresis, and Carbonate Extraction

Mitochondria isolated from yeast cells were stored in SEM buffer (250 mM sucrose, 1 mM EDTA, 10 mM MOPS-KOH, pH 7.2). Precursors were synthesized in the presence of [<sup>35</sup>S]methionine in reticulocyte lysate. Import reactions typically contained 5%–10% (v/v) reticulocyte lysate and 25–100  $\mu$ g mitochondria (protein amount). Import was performed at 25°C in import buffer (3% [w/v] BSA, 250 mM sucrose, 80 mM KCl, 5 mM MgCl<sub>2</sub>, 5 mM methionine, 10 mM KH<sub>2</sub>PO<sub>4</sub>, 10 mM MOPS-KOH, pH 7.2) containing 2–4 mM ATP, 2–4 mM NADH, 5 mM creatine phosphate, and 100  $\mu$ g/ml creatine kinase. The membrane potential was dissipated by addition of 8  $\mu$ M antimycin A, 1  $\mu$ M valinomycin, and 20  $\mu$ M oligomycin (final concentrations). Where indicated, 5  $\mu$ M methotrexate was added (final concentration). The import reaction was stopped by transfer on ice. Where indicated, nonimported precursors were removed by addition of 10–50  $\mu$ g/ml proteinase K. After import, mitochondria were washed with SEM buffer. To chase the precursor, mitochondria were further incubated in SEM buffer containing 4 mM ATP, 5 mM creatine phosphate, 100  $\mu$ g/ml creatine kinase, and 5 mM EDTA. Imported precursor proteins were detected by SDS-PAGE and autoradiography (Stojanovski et al., 2007). Alternatively, import samples were lysed with 1% (w/v) digitonin in lysis buffer (20 mM Tris-HCl, pH 7.4, 0.1 mM EDTA, 50 mM NaCl, 10% glycerol) and protein complexes were separated by BN electrophoresis. Membrane integration of proteins was assessed by treatment of mitochondria with 0.1 M Na<sub>2</sub>CO<sub>3</sub>, pH 11.5. Pellet and supernatant fractions were separated by centrifugation for 30 min at 125,000  $\times$  g (Thornton et al., 2010).

### Tracking of $\beta$ -Barrel Folding by Oxidation, Chemical Crosslinking, and Thiol Trapping

Isolated mitochondria in SEM buffer were treated with 0.2 mM 4,4'-dipyridyl disulfide (4-DPS), 2 mM Cu-phenanthroline (CuP; 80 mM CuP stock solution was freshly prepared by adding 2 vol 0.36 M 1,10-phenanthroline in 50%

ethanol to 1 vol 0.24 M CuSO<sub>4</sub>) or 2 mM CuSO<sub>4</sub> on ice for 10 min. The remaining free SH groups were blocked with 50 mM iodoacetamide for 10 min on ice (in case of CuP and CuSO<sub>4</sub> additionally 10 mM EDTA was added). After washing disulfide bonds were reduced with 50 mM DTT for 15 min at 30°C where indicated. Mitochondria were lysed under denaturing conditions followed by separation of the oxidized and reduced proteins by nonreducing SDS-PAGE. Chemical crosslinking was performed with 1 mM BMB, 1 mM 1,6-bis(maleimido)hexane (BMH), 1 mM BMOE, or 1 mM DSG for 30 min on ice (Pierce). Reactions were quenched by addition of 50 mM DTT for BMB, BMH, and BMOE, or 0.1 M Tris-HCl, pH 7.4, for DSG. Crosslinking with 1 mM M1M was performed for 30 min at 30°C and stopped by 50 mM iodoacetamide. For indirect thiol trapping, oxidized mitochondria were incubated with iodoacetamide at 30°C for 1 hr to block free cysteine residues; disulfide bonds were reduced by 50 mM DTT and treated with BMH, or mitochondria were lysed in 1% SDS supplemented with 2.5 mM methoxyl-polyethylene glycol-maleimide (mPEG-MAL 5 kDa; Nanocs).

### Affinity Purification

Mitochondria from strains expressing Protein A- or His-tagged proteins were lysed with 1% (w/v) digitonin in lysis buffer. After a clarifying spin, the supernatant was incubated with IgG-Sepharose or Ni-NTA agarose, respectively, for 1 hr at 4°C. The beads were washed and bound proteins were eluted by cleavage with tobacco etch virus protease (AcTEV; Invitrogen) or imidazole. Yeast cell extracts of WT, Sam50<sup>ProtA</sup>, and Sam37<sup>ProtA</sup> strains were lysed with 1% (w/v) digitonin in lysis buffer and incubated with IgG-Sepharose (Bohnert et al., 2012). Proteins present in affinity-purified SILAC-labeled Sam50 complexes were identified and quantified by ultra-high-performance liquid chromatography-tandem mass spectrometry and subsequent MaxQuant data analysis as described in detail in [Extended Experimental Procedures](#). Coimmunoprecipitation of arrested precursor was performed as previously described (Thornton et al., 2010).

### SUPPLEMENTAL INFORMATION

Supplemental Information includes Extended Experimental Procedures, six figures, and one table and can be found with this article online at <http://dx.doi.org/10.1016/j.cell.2013.06.033>.

### ACKNOWLEDGMENTS

We thank Drs. C. Meisinger and R. Ieva for discussion. This work was supported by the Deutsche Forschungsgemeinschaft, Sonderforschungsbereich 746, Excellence Initiative of the German Federal and State Governments (EXC 294 BIOS; GSC-4 Spemann Graduate School), Landesforschungspreis Baden-Württemberg, and Bundesministerium für Bildung und Forschung.

Received: February 15, 2013

Revised: May 13, 2013

Accepted: June 19, 2013

Published: August 1, 2013

### REFERENCES

- Becker, T., Gebert, M., Pfanner, N., and van der Laan, M. (2009). Biogenesis of mitochondrial membrane proteins. *Curr. Opin. Cell Biol.* *21*, 484–493.
- Becker, T., Guiard, B., Thornton, N., Zufall, N., Stroud, D.A., Wiedemann, N., and Pfanner, N. (2010). Assembly of the mitochondrial protein import channel: role of Tom5 in two-stage interaction of Tom40 with the SAM complex. *Mol. Biol. Cell* *21*, 3106–3113.
- Bohnert, M., Wenz, L.S., Zerbes, R.M., Horvath, S.E., Stroud, D.A., von der Malsburg, K., Müller, J.M., Oeljeklaus, S., Perschil, I., Warscheid, B., et al. (2012). Role of mitochondrial inner membrane organizing system in protein biogenesis of the mitochondrial outer membrane. *Mol. Biol. Cell* *23*, 3948–3956.
- Chacinska, A., Rehling, P., Guiard, B., Frazier, A.E., Schulze-Specking, A., Pfanner, N., Voos, W., and Meisinger, C. (2003). Mitochondrial translocation contact sites: separation of dynamic and stabilizing elements in formation of a TOM-TIM-preprotein supercomplex. *EMBO J.* *22*, 5370–5381.
- Dolezal, P., Likic, V., Tachezy, J., and Lithgow, T. (2006). Evolution of the molecular machines for protein import into mitochondria. *Science* *313*, 314–318.
- Dukanovic, J., and Rapaport, D. (2011). Multiple pathways in the integration of proteins into the mitochondrial outer membrane. *Biochim. Biophys. Acta* *1808*, 971–980.
- Endo, T., and Yamano, K. (2010). Transport of proteins across or into the mitochondrial outer membrane. *Biochim. Biophys. Acta* *1803*, 706–714.
- Ghaemmaghani, S., Huh, W.K., Bower, K., Howson, R.W., Belle, A., Dephoure, N., O'Shea, E.K., and Weissman, J.S. (2003). Global analysis of protein expression in yeast. *Nature* *425*, 737–741.
- Habib, S.J., Waizenegger, T., Niewianda, A., Paschen, S.A., Neupert, W., and Rapaport, D. (2007). The N-terminal domain of Tob55 has a receptor-like function in the biogenesis of mitochondrial  $\beta$ -barrel proteins. *J. Cell Biol.* *176*, 77–88.
- Hagan, C.L., Silhavy, T.J., and Kahne, D. (2011).  $\beta$ -Barrel membrane protein assembly by the Bam complex. *Annu. Rev. Biochem.* *80*, 189–210.
- Harner, M., Körner, C., Walther, D., Mokranjac, D., Kaesmacher, J., Welsch, U., Griffith, J., Mann, M., Reggiori, F., and Neupert, W. (2011). The mitochondrial contact site complex, a determinant of mitochondrial architecture. *EMBO J.* *30*, 4356–4370.
- Hewitt, V., Alcock, F., and Lithgow, T. (2011). Minor modifications and major adaptations: the evolution of molecular machines driving mitochondrial protein import. *Biochim. Biophys. Acta* *1808*, 947–954.
- Hoppins, S.C., and Nargang, F.E. (2004). The Tim8-Tim13 complex of *Neurospora crassa* functions in the assembly of proteins into both mitochondrial membranes. *J. Biol. Chem.* *279*, 12396–12405.
- Ishikawa, D., Yamamoto, H., Tamura, Y., Moritoh, K., and Endo, T. (2004). Two novel proteins in the mitochondrial outer membrane mediate  $\beta$ -barrel protein assembly. *J. Cell Biol.* *166*, 621–627.
- Klein, A., Israel, L., Lackey, S.W.K., Nargang, F.E., Imhof, A., Baumeister, W., Neupert, W., and Thomas, D.R. (2012). Characterization of the insertase for  $\beta$ -barrel proteins of the outer mitochondrial membrane. *J. Cell Biol.* *199*, 599–611.
- Krimmer, T., Rapaport, D., Ryan, M.T., Meisinger, C., Kassenbrock, C.K., Blachly-Dyson, E., Forte, M., Douglas, M.G., Neupert, W., Nargang, F.E., and Pfanner, N. (2001). Biogenesis of porin of the outer mitochondrial membrane involves an import pathway via receptors and the general import pore of the TOM complex. *J. Cell Biol.* *152*, 289–300.
- Kutik, S., Stojanovski, D., Becker, L., Becker, T., Meinecke, M., Krüger, V., Prinz, C., Meisinger, C., Guiard, B., Wagner, R., et al. (2008). Dissecting membrane insertion of mitochondrial  $\beta$ -barrel proteins. *Cell* *132*, 1011–1024.
- Meisinger, C., Ryan, M.T., Hill, K., Model, K., Lim, J.H., Sickmann, A., Müller, H., Meyer, H.E., Wagner, R., and Pfanner, N. (2001). Protein import channel of the outer mitochondrial membrane: a highly stable Tom40-Tom22 core structure differentially interacts with preproteins, small tom proteins, and import receptors. *Mol. Cell Biol.* *21*, 2337–2348.
- Model, K., Meisinger, C., Prinz, T., Wiedemann, N., Truscott, K.N., Pfanner, N., and Ryan, M.T. (2001). Multistep assembly of the protein import channel of the mitochondrial outer membrane. *Nat. Struct. Biol.* *8*, 361–370.
- Neupert, W., and Herrmann, J.M. (2007). Translocation of proteins into mitochondria. *Annu. Rev. Biochem.* *76*, 723–749.
- Paschen, S.A., Waizenegger, T., Stan, T., Preuss, M., Cyrklaff, M., Hell, K., Rapaport, D., and Neupert, W. (2003). Evolutionary conservation of biogenesis of  $\beta$ -barrel membrane proteins. *Nature* *426*, 862–866.
- Rapaport, D., and Neupert, W. (1999). Biogenesis of Tom40, core component of the TOM complex of mitochondria. *J. Cell Biol.* *146*, 321–331.
- Schmidt, O., Pfanner, N., and Meisinger, C. (2010). Mitochondrial protein import: from proteomics to functional mechanisms. *Nat. Rev. Mol. Cell Biol.* *11*, 655–667.

- Shiota, T., Maruyama, M., Miura, M., Tamura, Y., Yamano, K., Esaki, M., and Endo, T. (2012). The Tom40 assembly process probed using the attachment of different intramitochondrial sorting signals. *Mol. Biol. Cell* 23, 3936–3947.
- Stojanovski, D., Pfanner, N., and Wiedemann, N. (2007). Import of proteins into mitochondria. *Methods Cell Biol.* 80, 783–806.
- Stroud, D.A., Becker, T., Qiu, J., Stojanovski, D., Pfannschmidt, S., Wirth, C., Hunte, C., Guiard, B., Meisinger, C., Pfanner, N., and Wiedemann, N. (2011a). Biogenesis of mitochondrial  $\beta$ -barrel proteins: the POTRA domain is involved in precursor release from the SAM complex. *Mol. Biol. Cell* 22, 2823–2833.
- Thornton, N., Stroud, D.A., Milenkovic, D., Guiard, B., Pfanner, N., and Becker, T. (2010). Two modular forms of the mitochondrial sorting and assembly machinery are involved in biogenesis of  $\alpha$ -helical outer membrane proteins. *J. Mol. Biol.* 396, 540–549.
- Tommassen, J. (2010). Assembly of outer-membrane proteins in bacteria and mitochondria. *Microbiology* 156, 2587–2596.
- van Wilpe, S., Ryan, M.T., Hill, K., Maarse, A.C., Meisinger, C., Brix, J., Dekker, P.J.T., Moczko, M., Wagner, R., Meijer, M., et al. (1999). Tom22 is a multifunctional organizer of the mitochondrial preprotein translocase. *Nature* 401, 485–489.
- Walther, D.M., Rapaport, D., and Tommassen, J. (2009). Biogenesis of  $\beta$ -barrel membrane proteins in bacteria and eukaryotes: evolutionary conservation and divergence. *Cell. Mol. Life Sci.* 66, 2789–2804.
- Wiedemann, N., Kozjak, V., Chacinska, A., Schönfisch, B., Rospert, S., Ryan, M.T., Pfanner, N., and Meisinger, C. (2003). Machinery for protein sorting and assembly in the mitochondrial outer membrane. *Nature* 424, 565–571.
- Wiedemann, N., Truscott, K.N., Pfannschmidt, S., Guiard, B., Meisinger, C., and Pfanner, N. (2004). Biogenesis of the protein import channel Tom40 of the mitochondrial outer membrane: intermembrane space components are involved in an early stage of the assembly pathway. *J. Biol. Chem.* 279, 18188–18194.
- Yamano, K., Yatsukawa, Y., Esaki, M., Hobbs, A.E., Jensen, R.E., and Endo, T. (2008). Tom20 and Tom22 share the common signal recognition pathway in mitochondrial protein import. *J. Biol. Chem.* 283, 3799–3807.